Civil Engineering Infrastructures Journal xx,xx
DOI: 10.22059/ceij.2026.394749.2308

Numerical study on the cyclic response of suction bucket foundations in clay under one-way cyclic lateral loading

Cheddad, M.[1], Amrane, M.N.[2]* and Ouahab, M.Y.[3]

[1] Ph.D. Candidate, Hydraulic Planning and Environment Laboratory (LAHE)., University of Mohamed Khider, P.B. 145, 07000 Biskra, Algeria.

[2] Professor, Department of mechanics, University of Mohamed Khider P.B. 145, 07000 Biskra, Algeria.

[3] Associate Professor, Department of Civil Engineering, Tipaza University Center, 42000 Tipaza, Algeria.

* Corresponding author E-mail: mn.amrane@univ-biskra.dz

Received: 09/05/2025
Revised: 29/12/2025
Accepted: 12/02/2026

ABSTRACT: The cumulative plastic deformations induced by cyclic loading are a critical design consideration for bucket foundations of offshore wind turbines. While past research has extensively characterized foundation behavior under static loads, the combined effects of cyclic lateral loading and soil strength non-homogeneity remain underexplored. This study examines through numerical analyses the behavior of a bucket foundation in clay subjected to one-way cyclic lateral loads. The cumulative plastic deformation was modeled employing a nonlinear kinematic hardening constitutive model. A parametric study evaluated the influence of the strength non-homogeneity degree, cyclic load amplitude, cyclic load ratio, and the kinematic hardening degradation parameter. The results demonstrate that while cumulative rotation and displacement increase with the number of cycles and load amplitude, they are significantly mitigated by a greater degree of non-homogeneity. Increasing κ from 10 to 25 diminished rotation by 57% and horizontal and vertical displacements by 56% and 75%, respectively. The lowest cyclic load ratio produced the largest deformations, while a higher kinematic hardening degradation parameter resulted in the smallest deformations. Model validation against established experimental and numerical benchmarks shows good agreement. These results offer a useful understanding of the cyclic behavior of bucket foundations.

Keywords: Cyclic response; Bucket foundation; Cyclic lateral loading; Cumulative deformation; Clays.

1. Introduction

In offshore facilities, such as oil and gas platforms, offshore wind turbines, and jacket structures, bucket foundations have been widely utilized as an alternative to traditional systems of foundations like gravity foundations and monopile foundations.

The suction bucket foundation system has notable advantages regarding the high lateral

load carrying capacity, cost effectiveness, and installation efficiency. The suction bucket is a steel cylinder with an open bottom and a closed top that is installed by penetrating into the soil under its own weight. Once it reaches the desired depth, under-pressure (suction) is applied in the bucket to reach the intended penetration. The suction bucket foundations experience cyclic lateral loading induced by the action of environmental loads (wind, waves, currents). Cyclic loading can increase pore pressures in the soil; Pore pressure buildup diminishes effective stresses, resulting in reduced shear strength and stiffness in the soil and may lead to accumulated deformations (Andersen and Lauritzsen, 1988).

* Corresponding author E-mail:

displacements, and settlement of suction buckets are significantly influenced by soil conditions, bucket geometry, and parameters related to cyclic loading such as number of cycles, loading amplitude, and frequency. Hung et al. (2018) performed a 1g laboratory test to explore the accumulated rotation and unloading stiffness of two bucket models in clay under one-way cyclic loading. The results indicated that the accumulation of rotations increased with increasing number of loading cycles and cyclic load magnitude. An empirical equation was developed for bucket foundations in soft clays under one-way cyclic lateral loading to predict the accumulated rotations as well as the unloading stiffness.

Numerous finite element models have been conducted on the performance of suction bucket foundations subjected to cyclic loads (Kourkoulis et al., 2014; Cheng et al., 2018; Bagheri and Kim, 2019; Cheng et al., 2020; Barari et al., 2021; T. Wang et al., 2021; W. Zhou et al., 2021; Cheng et al., 2022; Yilmaz and Tasan, 2022; Roy et al., 2024; Song et al., 2025). However, this body of research has predominantly focused on homogeneous soil conditions or the modeling of plastic failure.

Several studies have explored the behavior of suction bucket foundations through field tests (Houlsby et al., 2005; X. Zhu et al., 2023) and model tests (B. Zhu et al., 2013; Nielsen et al., 2017; B. Zhang et al., 2020; Jeong et al., 2021; Lian et al., 2021; X. Wang et al., 2022; N. Zhou et al., 2022; Kou et al., 2023; Zayed et al., 2023). The findings of these tests indicated that the bearing capacity, unloading stiffness, cumulative rotations,

Cheng et al. (2022) examined the effects of bucket-soil contact conditions, cyclic loading modes, and direction of the applied cyclic loading on the cyclic responses of tripod suction bucket foundations using a three-dimensional finite element model through an elastoplastic single bounding surface constitutive model.

Cheng et al. (2020) developed a novel numerical method to model the cyclic behavior of suction anchors in soft clay. Their approach combines both an elastic-perfectly plastic Mohr-Coulomb constitutive model and a custom stiffness degradation model, calibrated from undrained cyclic triaxial tests. Incorporated into ABAQUS via a user-defined subroutine, this coupled framework captures the degradation of stiffness and the accumulation of plastic deformation surrounding the anchor subjected to both combined average and cyclic loads.

Cheng et al. (2018) established and implemented a specialized bounding surface elastoplastic model via a UMAT subroutine to numerically model the cyclic response.

Their study combined physical model tests under 1g conditions with advanced 3D finite element analysis. The results demonstrated that this approach can effectively model the complete cyclic deformation process, accurately predict displacement-time histories, load-displacement hysteresis, failure modes, and cyclic bearing capacity of suction

anchors in soft clay.

Bagheri and Kim (2019) demonstrated that both bucket geometry and soil properties are significant, with soil density having a greater effect on foundation response than geometry. Their analysis revealed that smaller buckets embedded in medium-dense soil exhibited the lowest initial stiffness, which further degraded progressively with cyclic loading compared to larger geometries.

Kourkoulis et al. (2014) specifically investigated the effect of both soil–sidewall interface strength and soil non-uniformity on the caisson response under monotonic, cyclic, and seismic loading, employing a nonlinear kinematic hardening model. Despite these advances, a systematic investigation into the effect of soil strength non-homogeneity on the progressive accumulation of plastic strains under cyclic loading, which is an essential consideration for the foundation design of offshore wind turbines, remains absent from the literature. This study aims to address this specific gap.

The cumulative rotations caused by cyclic loading represent an important factor in the design process for bucket foundations (B. Zhu et al., 2013), which must remain within specified serviceability thresholds. In the design of the Thornton Bank wind farm foundations, the allowable limit for structural rotation was 0.25º (Peire et al., 2009). The Chinese design code recommends that the cyclic cumulative rotation remain below 0.17° (Hydropower and Water Resources Planning and Design General Institute, 2008).

It is commonly known that soils can undergo plastic deformations at stress levels beneath the limit state threshold (Al-Janabi and Aubeny, 2022).

Standard methods for estimating the deformation of caissons in clay were established using linear elastic and elastoplastic soil models, which consider elastic response for stresses level under the maximum yield stress. Consequently, these models do not capture accumulative plastic displacements when cyclic stress amplitudes are much smaller than the maximum yield stress , allowing inelastic deformations to develop only when the maximum stress is reached. As a result, the prediction of cumulative displacements based on these models does not accurately depict the nonlinear cumulative permanent behavior of soil (Al-Ramthan and Aubeny, 2020). These constraints can be resolved by using a kinematic hardening constitutive model from the ABAQUS code.

The current work aims to investigate the response of the bucket foundation of an offshore wind turbine in clay soil subjected to one-way cyclic lateral loading. A kinematic hardening constitutive model is used to model cumulative plastic deformations while the applied loads are beneath the bucket foundation's ultimate load capacity.

2. Methodology

A simplified kinematic hardening constitutive model was employed to model the cumulative plastic deformation at stress levels below the limit threshold and for a completely undrained response. The model exists in Abaqus code and has been extensively employed to model cyclic and seismic soil structure interaction (Kourkoulis et al., 2014; Al-Ramthan and Aubeny, 2020; Saleh Asheghabadi and Cheng, 2020; J. Zhang et al., 2021; Al-Janabi and Aubeny, 2022). The analysis was performed for cohesive soils under undrained conditions; therefore, the accumulation and dissipation of pore-pressure were not modeled. Therefore, the presented analyses model a strictly undrained, non-consolidating condition where the total volume of the soil skeleton is constrained, but the internal pore pressure evolution is not explicitly calculated.

This model can offer a simplified framework to estimating the plastic deformations accumulated induced by cyclic loading (Al-Ramthan and Aubeny, 2020).

The objective of the current work is to explore the cyclic response of a suction bucket foundation used for offshore wind turbine installed in clay under one-way cyclic loading.

The research specifically focuses on quantifying the effects of key parameters related to soil properties, cyclic loading characteristics, and the constitutive model on the foundation's cumulative rotations and displacements, which are critical design considerations for long-term serviceability.

The clay-bucket foundation interaction was modeled in ABAQUS by means of a 3D finite element approach. To enhance computational efficiency, a half-symmetry model was employed, justified by the geometric and loading symmetry of the problem.

The model geometry in the numerical analysis was based on the dimensions typically used in analogous studies of offshore wind turbine (OWT) suction caissons. For instance, parametric studies by Kourkoulis et al. (2014) examined models with diameters D of 20 m and 25 m and skirt lengths L ranging from 4 m to 10 m for turbine towers of H = 60 m and 80 m. Similarly, T. Wang et al. (2021) utilized a diameter of 20 m with lengths of 10 m and 20 m. More recently, a benchmark study by J. Zhang et al. (2021) employed a bucket foundation with D = 20 m, L = 10 m, and H = 90 m for a 3.5 MW Offshore Wind Turbine model. Within this established framework, the present study adopts a representative baseline geometry of D = 20 m, L = 15 m, and H = 90 m. This configuration was selected as a central, practical case (with an L/D ratio of 0.75, falling between the ratios in the cited literature) to serve as the subject of a detailed parametric analysis in this study.

The parameters investigated include the strength non-homogeneity degree, cyclic load amplitude, cyclic load ratio, and the parameter controlling the reduction in kinematic hardening with increased plastic deformation.

The dimensions of the finite element soil domain were selected to minimize boundary effects on the foundation's response. A domain size of 6D in width and 3D in depth was adopted (Fan et al., 2020). This geometry is close to the 6D × 2.5D domain used by Kourkoulis et al. (2014).

Constitutive model

The analysis utilizes the nonlinear kinematic hardening model proposed by Lemaitre and Chaboche (1990), a formulation that originates from the study of Armstrong and Frederick (1966), which incorporates a Von Mises yield criterion and is available in ABAQUS. This constitutive framework is capable of predicting ratcheting behavior under cyclic loading.

The uniaxial compression strength of the soil, σ_{max}, determines the limit surface. According to the von Mises criterion, the uniaxial strength is given by:

$$\sigma_{max} = \sqrt{3}\, S_u \quad (1)$$

The stress evolution is defined according to Anastasopoulos et al. (2011)

$$\sigma = \sigma_0 + \alpha \quad (2)$$

In which σ_o represents the stress at zero plastic strain, and α refers to the backstress. While the kinematic evolution of the yield surface in the stress space is governed by this backstress.

The function F defines the yield surface (Chaboche, 2008):

$$F = f(\sigma - \alpha) - \sigma_0 \quad (3)$$

In which f(σ-α) represents the equivalent Mises stress with respect to the backstress α.

The flow rule for plastic deformation is formulated as follows (Chaboche, 2008):

$$\dot{\varepsilon}^{\mathrm{pl}} = \dot{\bar{\varepsilon}}^{\mathrm{pl}} \frac{\partial F}{\partial \sigma} \quad (4)$$

Where $\dot{\varepsilon}^{\mathrm{pl}}$ represents the plastic flow rate. $\dot{\bar{\varepsilon}}^{\mathrm{pl}}$ denotes the equivalent plastic strain rate.

In this model, there are two components that govern the evolution of stress: the isotropic hardening component and the Kinematic hardening component (Figure 1).

The isotropic hardening component accounts for changes in the equivalent stress, defining the yield surface size σ_0 in relation to plastic deformations.

$$\sigma_0 = \sigma_0 + Q_\infty(1 - e^{-b\bar{\varepsilon}^{pl}}) \quad (5)$$

Where Q_∞ and b represent model parameters describing the maximum variation in the yield surface size and the rate of this change with plastic strain, respectively.

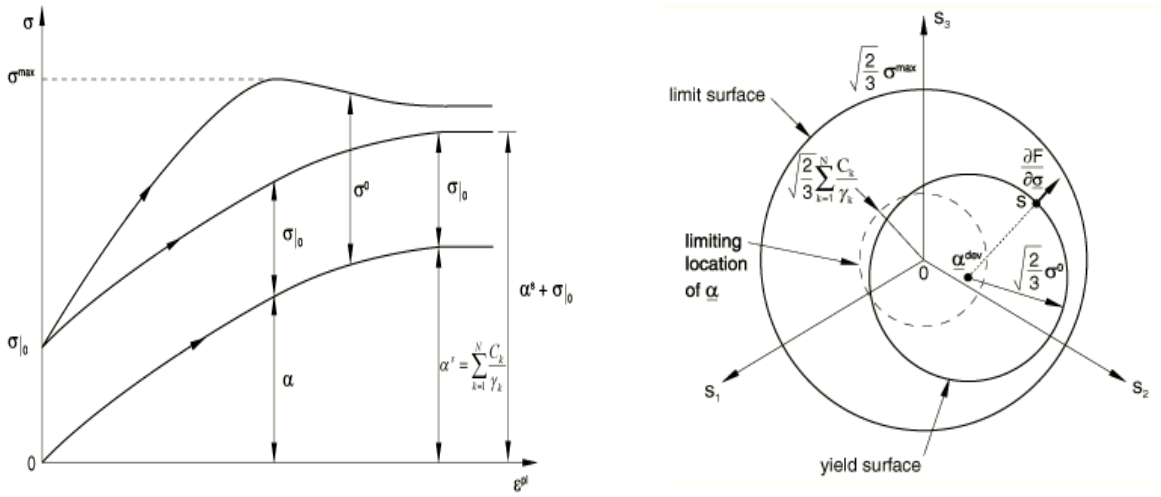

Fig. 1. Nonlinear isotropic/kinematic model: (a) one-dimensional and (b) three-dimensional representation of isotropic and kinematic hardening (Systèmes, 2016).

In this study, the yield stress is taken as constant, and only kinematic hardening is taken into consideration.

The Kinematic hardening component governs the yield surface translation within the stress space through the backstress parameter.

The evolution of the kinematic component of the yield stress is expressed according to the formulation:

$$\dot{\alpha} = C\frac{1}{\sigma_0}(\sigma - \alpha)\dot{\bar{\varepsilon}}^{\mathrm{pl}} - \gamma\alpha\dot{\bar{\varepsilon}}^{\mathrm{pl}} \qquad (6)$$

The equation derives from Ziegler's (1959) kinematic hardening formulation, extended with the nonlinear 'recall' term $\gamma\alpha\dot{\bar{\varepsilon}}^{pl}$ introduced by Lemaitre and Chaboche (1990).

γ can be obtained by the following equation:

$$\gamma = \frac{\mathrm{C}}{\sigma_{\max} - \sigma_0} \qquad (7)$$

Where σ_0 is the parameter controlling the beginning of the nonlinear response, expressed as a ratio λ of the yield stress σ_{max}. The value of λ ranges from 0.1 to 0.3 (Anastasopoulos et al., 2011).

Therefore, the γ parameter is determined from the following equation:

$$\gamma = \frac{C}{(1-\lambda)\sqrt{3}\ S_u} \qquad (8)$$

Where, C is the initial kinematic hardening modulus (in our case, we set it equal to the elastic modulus E) (Anastasopoulos et al., 2011).

γ is a parameter that defines the decreasing rate of kinematic hardening with increasing plastic deformation (the kinematic hardening degradation parameter).

3. Validation of the model with an experimental study

The finite element model was validated by comparing the numerical results with those obtained from the field test reported by Houlsby et al. (2005), as well as with the results of the experimental test and numerical analysis performed by Chen (2013). These benchmark studies were also used by T. Wang et al. (2021) for validation.

The field test was carried out at the Bothkennar field with a suction caisson foundation, with a diameter equal to 3m and with a skirt length of 1.5 m.

The soil's undrained shear strength is S_u=11.43+1.9Z, the young modulus is E=525 S_u, and the unit weight is 16.8 kN/m^3. The caisson mass (appurtenances included) is 2000 kg. The vertical load on the caisson was augmented by a 2400 kg block at the top of the A-frame of 4.23 m connected to the lid. A quasi-static cyclic load was applied by a hydraulic jack. To take into account the effect of the disturbance of the caisson installation on the soil. Houlsby et al. (2005) suggested a reduction factor of α= 0.5.

To verify the adopted numerical modelling, the results from the numerical analysis are compared with the test results. Figure 2 illustrates the relationship between the bending moment and the angular rotation at the center of the bucket lid. The numerical results reveal that the model successfully captures the hysteretic behavior of the response. In the first cycle, the model overpredicts positive rotation by 104.5% (5.89×10^{-4} rad against experimental 2.88×10^{-4} rad), suggesting initial overestimation of rotational deformability in this loading direction. This overestimation primarily arises because the non-linear kinematic model underestimates post-yield rotational stiffness during first-cycle initial loading. Upon load reversal, the high elastic stiffness governs reloading, while the translated yield surface (kinematic hardening) ensures that the subsequent cyclic response accurately matches the experimental behavior of the clay soil. The negative rotation shows better agreement with only 25.0% overprediction. The second cycle demonstrates improved correlation, with errors reducing to 15 to 22%. The model predicts positive peak rotations of 0.00163 rad, which are approximately 18% higher than the experimental peak. A quantitative analysis confirms a strong statistical correlation for the rotation, yielding a coefficient of determination of R^2 = 96.69%. Thus, the numerical results show good consistency with those of the test. Which proves the capability of the numerical method to capture the cyclic response of the suction bucket foundation.

Chen (2013) carried out 1-g model tests and also performed a finite element modeling to study suction caissons under undrained static lateral loading. Both the material and geometric characteristics of the suction caisson and the clay are provided in Table1.

Figure 3 compares the load-displacement curves from the finite element (FE) analysis with those from the experimental centrifuge test and other numerical modelling.

The present FE results demonstrate strong correlation with the experimental findings, with a coefficient of determination R^2 of 93.43%. They also show good correlation with the numerical analysis results from Chen (2013) and T. Wang et al. (2021), which themselves exhibited correlation coefficients of 88.56% and 88.64% with the experiment, respectively.

Table 1. Parameters of the experimental model test (Chen, 2013).

Parameter	Value
Caisson diameter, D (m)	0.1524
Caisson length L(m)	0.1524
Eccentricity of applied load, h (m)	0.9144
Saturated bulk unit weight γsat (kN/m3)	16.2835
Undrained shear strength Su (Kpa)	2.1546
Young's modulus, E (kPa)	300 S_u
Adhesion coefficient, α	0.8
Poisson's ratio, v	0.495

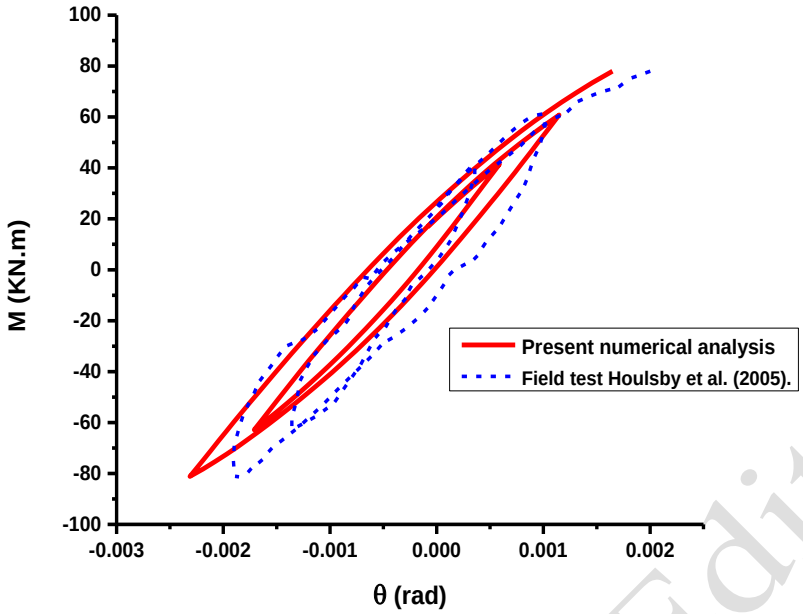

Fig. 2. Validation with a field test, Houlsby et al. (2005).

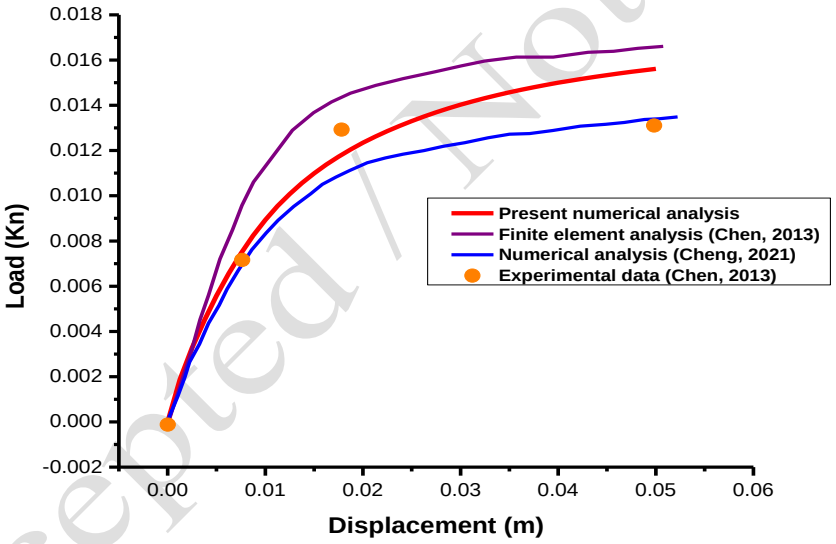

Fig. 3. Comparison of load-displacement curves from experimental data, a previous numerical study, and the present numerical model.

4. Finite-Element Modelling

In the present study, a finite-element model for a suction bucket foundation was developed to investigate its behavior in clay soil.

A three-dimensional finite element software program, ABAQUS, is used. As a result of geometric and loading symmetry, only half of the model was established , as demonstrated in Figure 4.

The bucket foundation has a diameter with size D= 20 m and a length of L=15 m. The height of the rotor is H= 90 m. The soil domain has a length and height of 6D and 3D. This configuration aligns with previous studies in the literature, specifically the work of Fan et al. (2020) and Kourkoulis et al. (2014). To verify the sufficiency of this domain size for cyclic analysis, a comparative model with an extended domain (10D laterally, 5D vertically) was analyzed under representative cyclic loading (ζ_b = 40%). As shown in Figure 5, the difference in cumulative rotation after 30 cycles was 1.41%, confirming that boundary effects

have a negligible influence on the global cyclic behavior.

The soil is discretized by **23052** eight -node linear brick elements with reduced integration **(C3D8R)** (T. Wang et al., 2021; Panwar and Dutta, 2023; Ghandi et al., 2025).

A mesh sensitivity study was performed to ensure numerical convergence. Three meshes with global element sizes were tested for a cyclic lateral loading case: coarse, medium (the selected mesh), and fine. The results for accumulated rotation over the first 30 cycles from the selected (medium) mesh differed by less than 0.04% from those of the finest mesh. Reduced-integration elements were chosen to mitigate shear locking in the undrained soil, and hourglass control was activated. Nonlinear analyses employed the default Full Newton-Raphson method. Convergence for each load increment was achieved when the force residual tolerance (0.5% of the time-averaged force norm) and the displacement correction tolerance (1% of the total displacement increment) were both satisfied, ensuring precise numerical equilibrium.

The bucket was modelled as shell elements with very high elastic modulus ($E=1\times 10^6$ Gpa) to consider the rigid behavior due to the use of stiffeners, and using a Poisson's ratio of 0.3. A sensitivity analysis on this rigidity assumption was conducted to verify that the global conclusions were not dependent on an idealized rigid structure. For a representative case (κ = 17.988, ζ_b = 40%), the Young's modulus was reduced to a realistic value for stiffened steel (E = 210 GPa) and an intermediate value ($E = 10^4$ GPa), and the cyclic analysis was repeated.

The results showed that the accumulated rotation after 30 cycles differed by less than 0.13% from the rigid case ($E = 10^6$ GPa). Furthermore, the fundamental attenuation behavior remained unchanged.

The bucket thickness is taken equal to t_{lid}=0.12 m. The skirt thickness is equal to t_{skirt}=0.04 m. Vertical boundaries were fixed against displacement in the horizontal normal direction; the bottom boundary was fixed in all directions.

The surface-to-surface contact method was used for modelling the interaction between the suction bucket and the surrounding soil due to the method's accuracy (Debnath and Pal, 2025).

The bucket foundation's surface is designated as the master surface , while the surface of the soil is assigned as the slave surface. Hard contact was set in the direction normal to the contact surface, which permitted separation between interface elements when they are exposed to tension.

For the tangential direction, the penalty contact method was adopted. When the two surfaces were in contact, the interface behavior was governed by Coulomb's friction theory.

At the contact surface, The critical frictional shear stress τ_{crit} can be written as $\tau_{crit}=\mu.p_c$ as a function of friction coefficient and contact pressure pc. İn the analyses, the friction coefficient is taken equal to μ=0.28. When the shear stress at the contact surface

surpassed the limit τ_{crit}, tangential slip happened. To consider the dead weight of the offshore wind turbine superstructure and the bucket foundation, a vertical load of 8.45 MN was applied at point A , as shown in Figure 4. Cyclic horizontal loading was also applied at the same point.

The soil is a saturated Kaolin clay. The parameters characterizing the soil are given in Table 2.

For marine clay, the undrained shear strength changes linearly as a function of depth (Ouahab et al., 2020; Shen et al., 2021; Shiva Bhushan et al., 2021; Keawsawasvong, 2022; Xiao et al., 2022; Shiva Bhushan et al., 2023), which is described by:

$$S_u = S_{um} + k.z \quad (9)$$

Where k is the gradient of strength, z indicates the depth within the soil.

The degree of non-homogeneity is given by a dimensionless ratio:

$$\kappa = \frac{k\,D}{S_{um}} \quad (10)$$

In which S_{um} is the undrained shear strength at mudline, and D is the foundation diameter.

For the kinematic hardening model, the value of $\frac{E}{S_u}$ is calculated by means of the parameters of the soil presented in Table 2.

The model's input parameters are as follows: λ=0.1, γ=173.33, Q=0, b=1.

For considering the effect of installation disturbance, a coefficient of adhesion factor is taken as α=0.8.

Table 2. Soil parameters for numerical analysis (Feng and Gourvenec, 2016).

Parameter	Value
Saturated bulk unit weight γ_{sat} (kN/m^3)	16
Recompression index κ	0.044
Vergin compression index λ	0.205
Stress ratio at critical state M	0.92
Intercept on critical state line (CSL), esc (at p'=1)	2.14
Poisson ratio ν	0.3
Wet yield surface size, β	1
Flow stress ratio K	1
Permeability of soil k (m/s)	1×10^{-9}
Undrained shear strength S_u (Kpa)	1.431+1.717 Z
Consolidation coefficient c_{v0} (m^2/s)	7.16×10^{-9}
Unit weight of water γ_{water} (kN/m3)	10

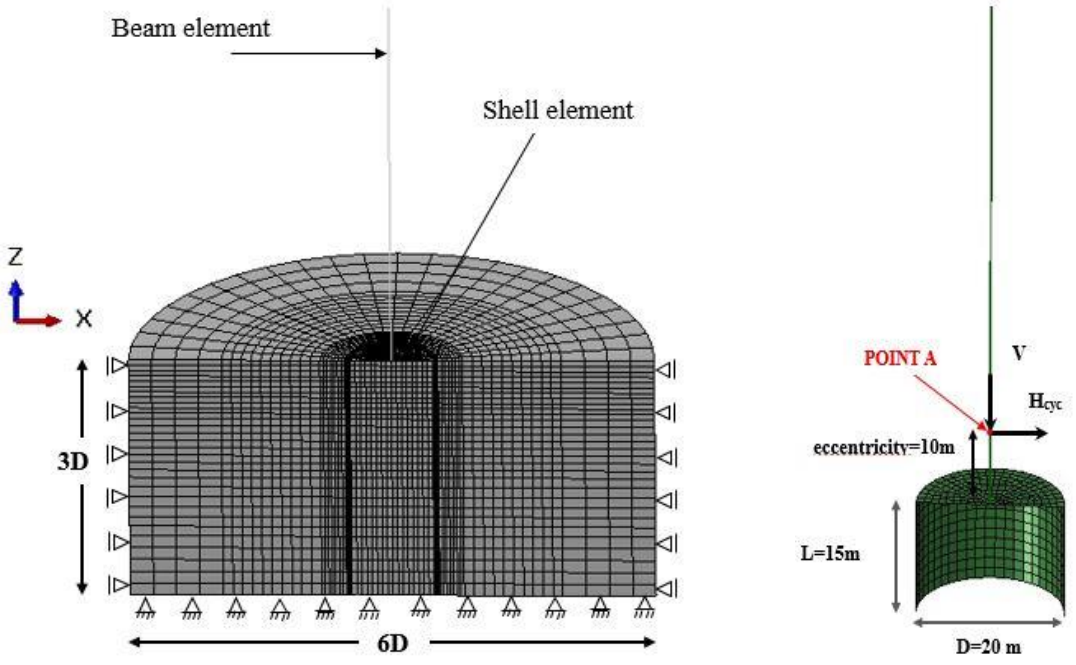

Fig. 4. Finite element meshing.

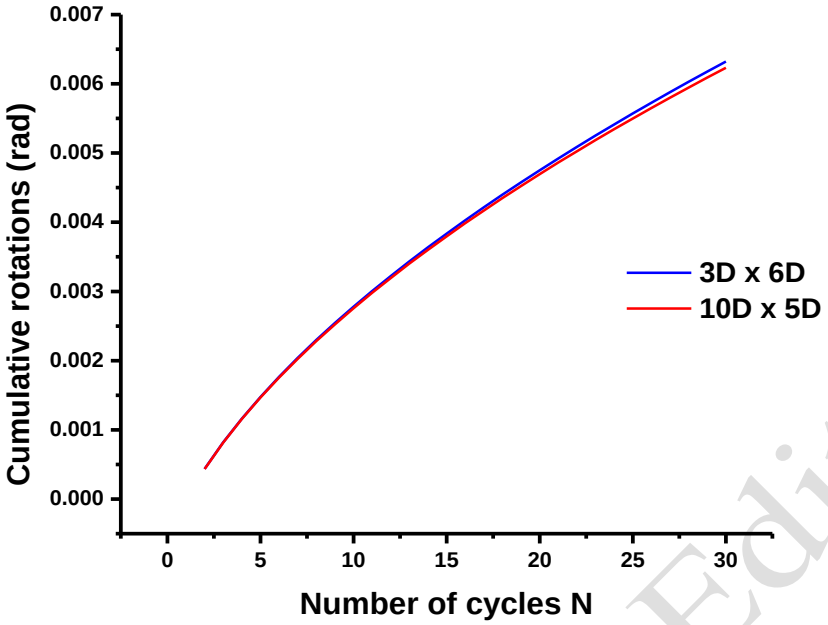

Fig. 5. Boundary effect sensitivity analysis: cumulative rotation versus number of load cycles for two soil domain sizes (6D × 3D and 10D × 5D).

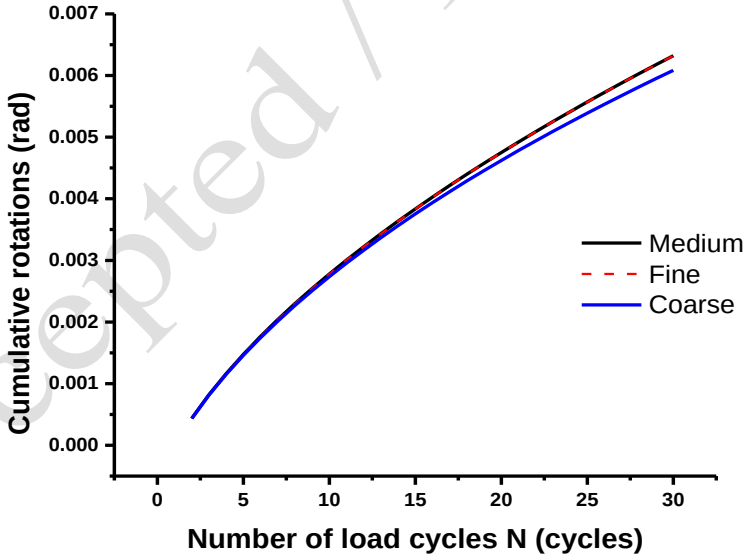

Fig. 6. Comparison of analysis results for the current, finer, and coarser meshes.

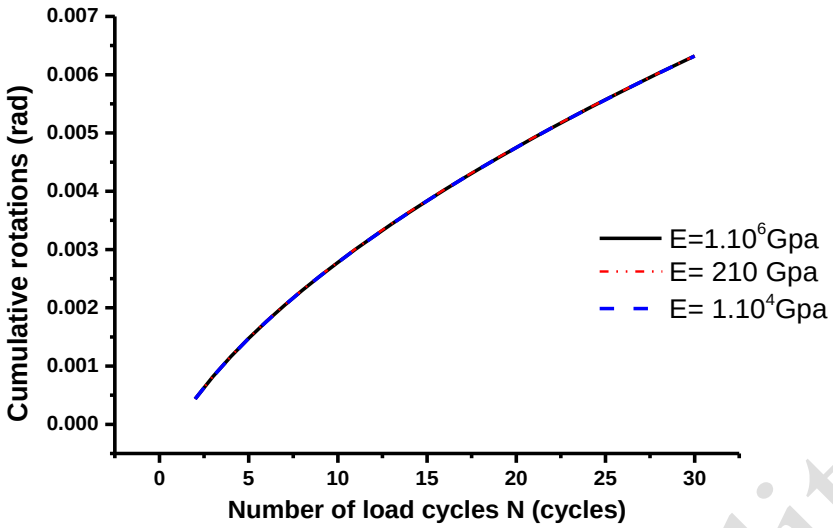

Fig. 7. Stiffness sensitivity analysis: cumulative rotation versus number of load cycles for three values of the bucket Young's modulus (E = 10^6 GPa, 10^4 GPa, and 210 GPa).

5. Parametric Study

Using the same material and geometrical properties as described in section 4, a parametric analysis was carried out to estimate the cumulative deformations under one-way cyclic loading with a period of T=10s (Figure 8). Taking into account parameters related to the soil properties, such as the strength non-homogeneity degree κ, number of load cycles N, and two parameters ζ_b and ζ_c (Figures 9 and 10) that define the characteristic of cyclic loading expressed as follows (LeBlanc et al., 2010):

$$\zeta_b = \frac{H_{max}}{H_{ult}} \tag{11}$$

$$\zeta_c = \frac{H_{min}}{H_{max}} \tag{12}$$

Where H_{ult} represents the suction bucket foundation's ultimate capacity.

H_{max}: Maximum loading amplitude.

H_{min}: Minimum loading amplitude.

The different undrained shear strength profiles adopted for the analysis are summarized in Table 3. In the parametric study, the ultimate capacity and the applied loads employed are listed in Table 4, with values provided for different strength non-homogeneity degrees κ and cyclic load amplitude ζ_b.

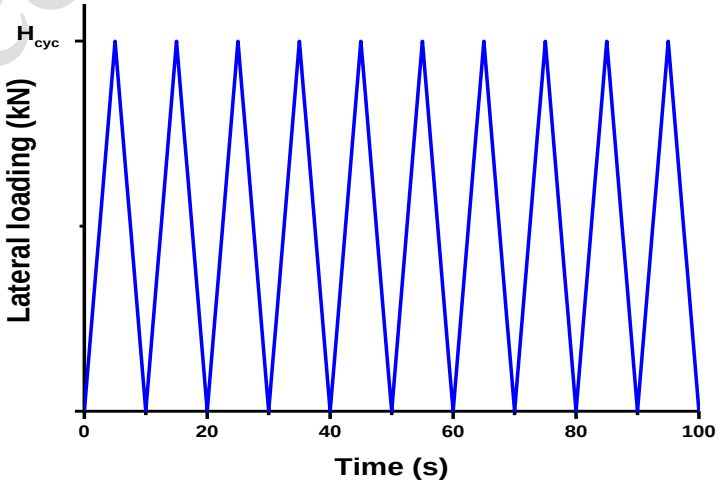

Fig. 8. One-way lateral cyclic loading.

Table 3. Undrained shear strength used in the parametric study.

κ	S_{u0}	k
10	1.908	0.954
15		1.431
17.998		1.717
20		1.908
25		2.385

Table 4. Lists of applied loads considered in the parametric study.

Degree of strength non homogeneity κ	Cyclic load amplitude ζ_b	Applied load H_{cyc} (kN)	Ultimate capacity H_{ult} (kN)
κ =10	50%	2880	5760
	40%	2304	
	30%	1728	
κ =15	50%	3880	7760
	40%	3140	
	30%	2328	
κ =17.998	50%	4320	8640
	40%	3456	
	30%	2592	
κ =20	50%	4500	9000
	40%	3600	
	30%	2700	
κ =25	50%	5050	10100
	40%	4040	
	30%	3030	

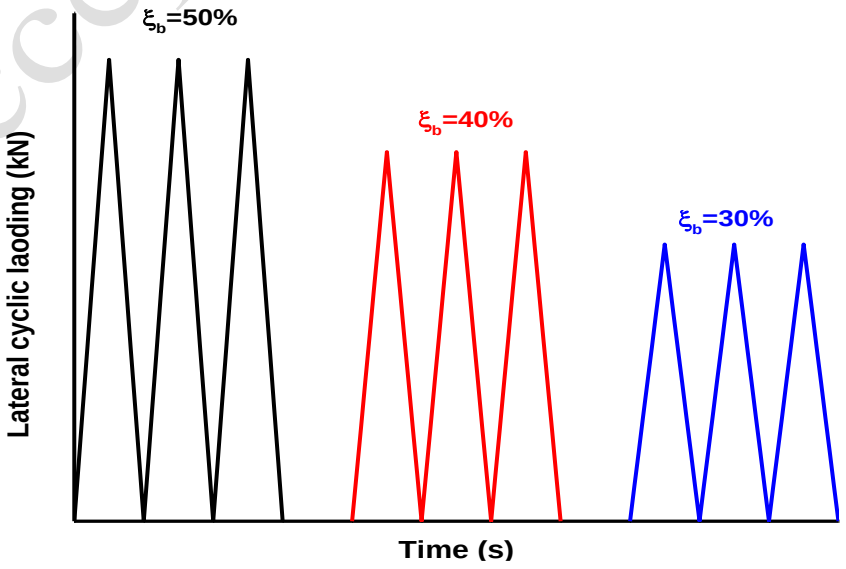

Fig. 9. One-way cyclic loading with different values of load amplitude parameter.

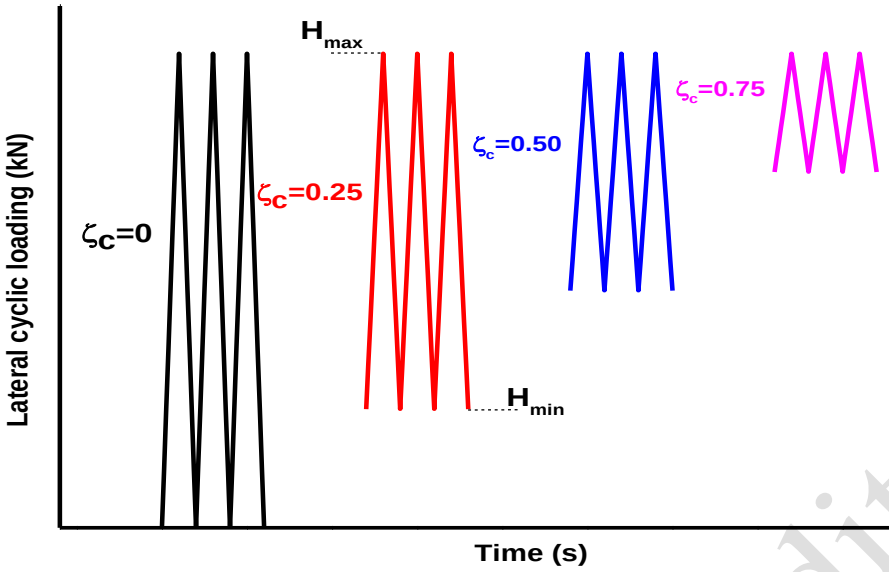

Fig. 10. One-way cyclic loading with different values of load symmetry parameter.

6. Results and Discussion

6.1 Effect of Strength non-homogeneity κ

Figure 11 (a-c) shows the effect of the strength non-homogeneity degree on the response of the bucket foundation against the number of load cycles, considering a range of values of κ from 10 to 25 and with cyclic load amplitude ζ_b=50% from the ultimate capacity.

Both cumulative rotations and displacements exhibited attenuation response, characterized by a nonlinear increase, where the accumulation rate decays gradually with increasing number of load cycles (Goldscheider and Gudehus, 1976). The rate of increase is significant for a low number of cycles (N≤20), followed by progressive diminution thereafter.

Furthermore, the analyses show that the bucket in the clay with the lowest strength non-homogeneity experienced the highest cumulative rotations and displacements. This occurs because during each reloading phase, soil with lower strength non-homogeneity experiences larger incremental plastic deformations. The fundamental reason is that greater strength non-homogeneity generates an intrinsically stiffer cyclic soil response, which limits progressive plastic deformation (ratcheting).

Figure 11 (c) presents the cumulative vertical displacements as a function of the number of loading cycles for various values of the strength non-homogeneity degree.

Obviously, with an increasing number of loading cycles, the cumulative vertical displacements rise progressively with a nonlinear, attenuating pattern.

Further, a greater strength non-homogeneity degree results in a reduction in cumulative vertical displacements. Increasing the strength non-homogeneity degree κ from 10 to 25 significantly reduces cumulative deformations, decreasing rotation, lateral displacement, and vertical displacement by approximately 57.07%, 55.60%, and 74.73%, respectively. This substantial reduction demonstrates that κ has a pronounced effect on the foundation's cyclic response. This stiffening effect occurs because a higher κ profile restricts the accumulation of plastic strain per cycle, thereby suppressing the ratcheting mechanism.

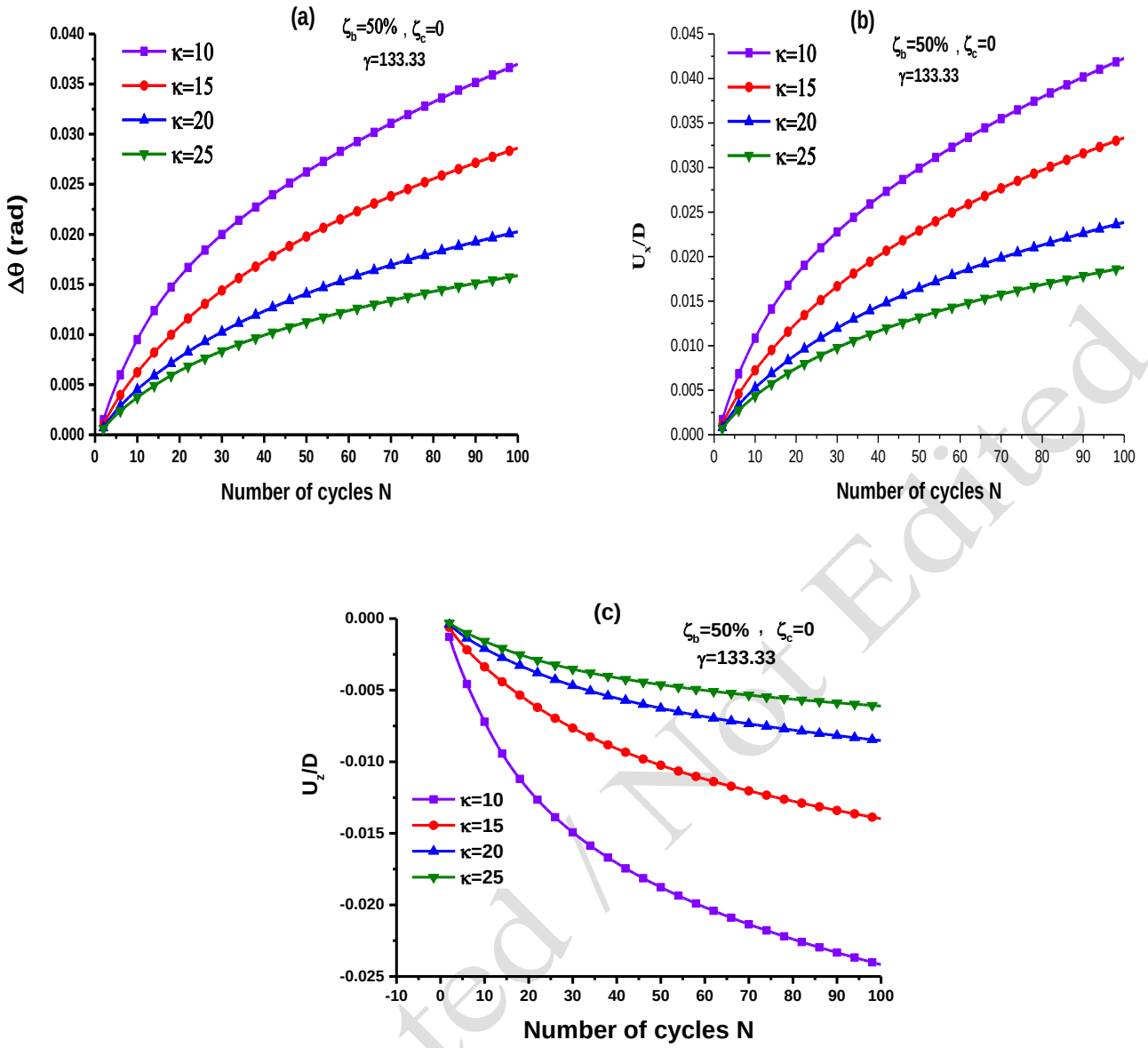

Fig. 11. Effect of degree of strength non-homogeneity on bucket foundation behavior: (a) cumulative rotations, (b) lateral displacements at the point A, (c) vertical displacements at the point A.

The displacement contours for the range values of the strength non-homogeneity degree are illustrated in Figure 12 (a-d) for a number of load cycles N=100. From these figures, it is noted that the largest displacements are concentrated in the right interior corner of the bucket close to the lid. The reason is that as the bucket foundation experiences cyclic loading, with the increased number of load cycles, the bucket skirt supports the majority of the loads, while the bucket lid supports a smaller part (Bagheri and Kim, 2019).

As illustrated in Figure 12 (a-d), with increasing strength non-homogeneity degree, the caisson's displacements in the lateral and downward directions become smaller and more confined. This behavior arises primarily because greater strength non-homogeneity increases the soil's stiffness, thereby restricting plastic deformation development. This mechanism is confirmed by the plastic strain contours, which show a more confined pattern in more non-homogeneous soil.

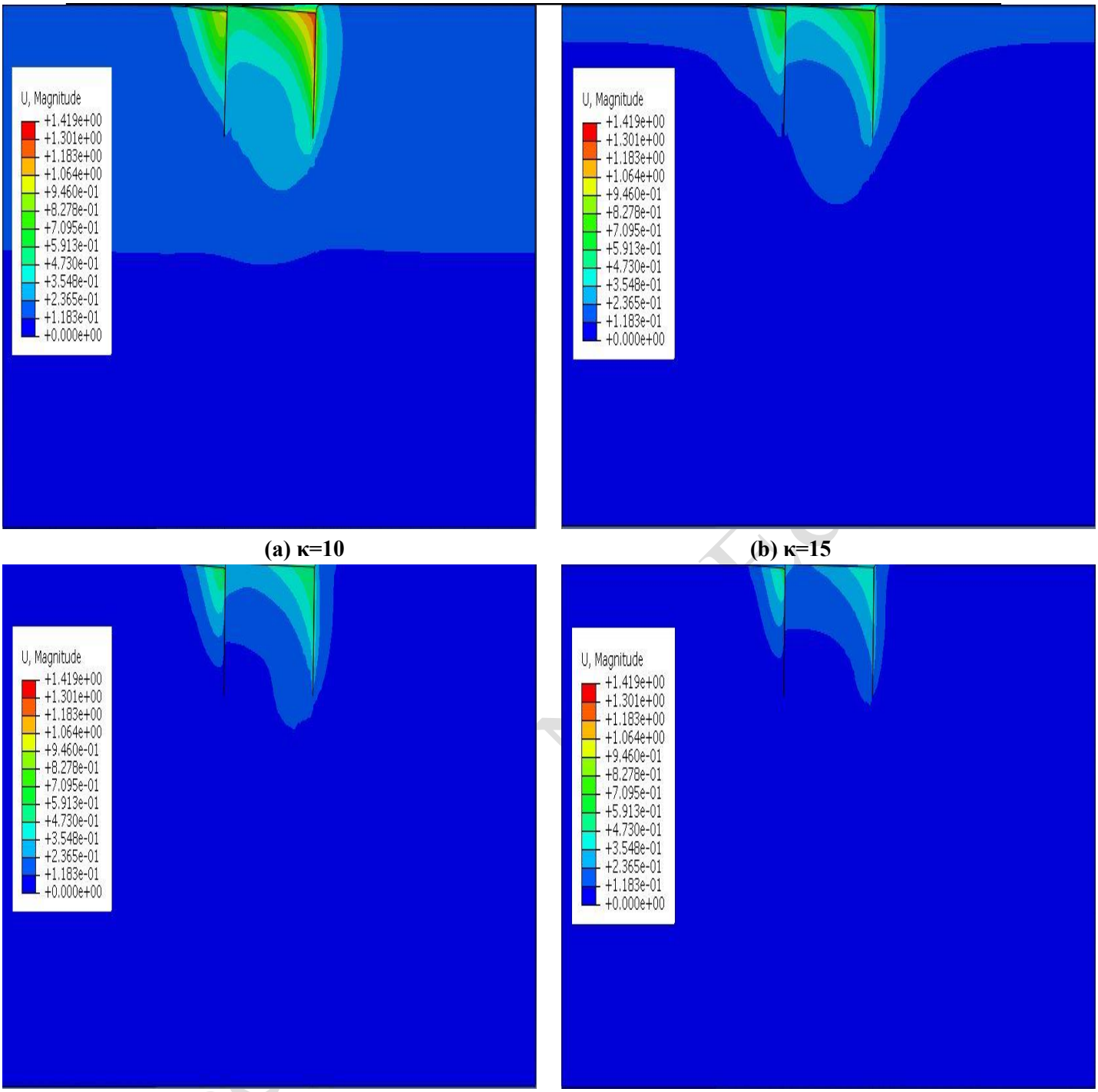

(a) κ=10 **(b) κ=15**

(c) κ=20 **(d) κ=25**

Fig. 12. Displacement contours for different values of degree of strength non-homogeneity and with N=100, ζ_b=50%, ζ_c=0.

6.2 Effect of cyclic load amplitude ζ_b

The evolution of cumulative rotations and cumulative displacements at different values of cyclic load amplitude ζ_b, against the number of load cycles N, is plotted in Figures 13(a-c). Cumulative rotations and displacements increase with both the number of load cycles and the cyclic load amplitude ζ_b. A consistent ratcheting mechanism is observed, where plastic strains accumulate progressively with each cycle, leading to a progressive increase in all deformation components. Crucially, the rate of accumulation is non-linear; the curves exhibit a declining slope, indicating a trend towards cyclic attenuation. This is primarily due to soil particle rearrangement and densification around the bucket.

Figure 13 (c) exhibits the cumulative vertical displacements of point A against the number of cycles N, accounting for various loading amplitudes. Obviously, A higher loading amplitude generates a larger cumulative vertical displacement.

An increase in the cyclic load amplitude ζ_b from 30% to 50%, the cumulative rotations increase about 307.49% while the cumulative lateral and vertical displacements increase about 311.25% and 183.09%, respectively. This observation implies that cyclic load amplitude ζ_b has a significant effect on cumulative rotations and cumulative displacements.

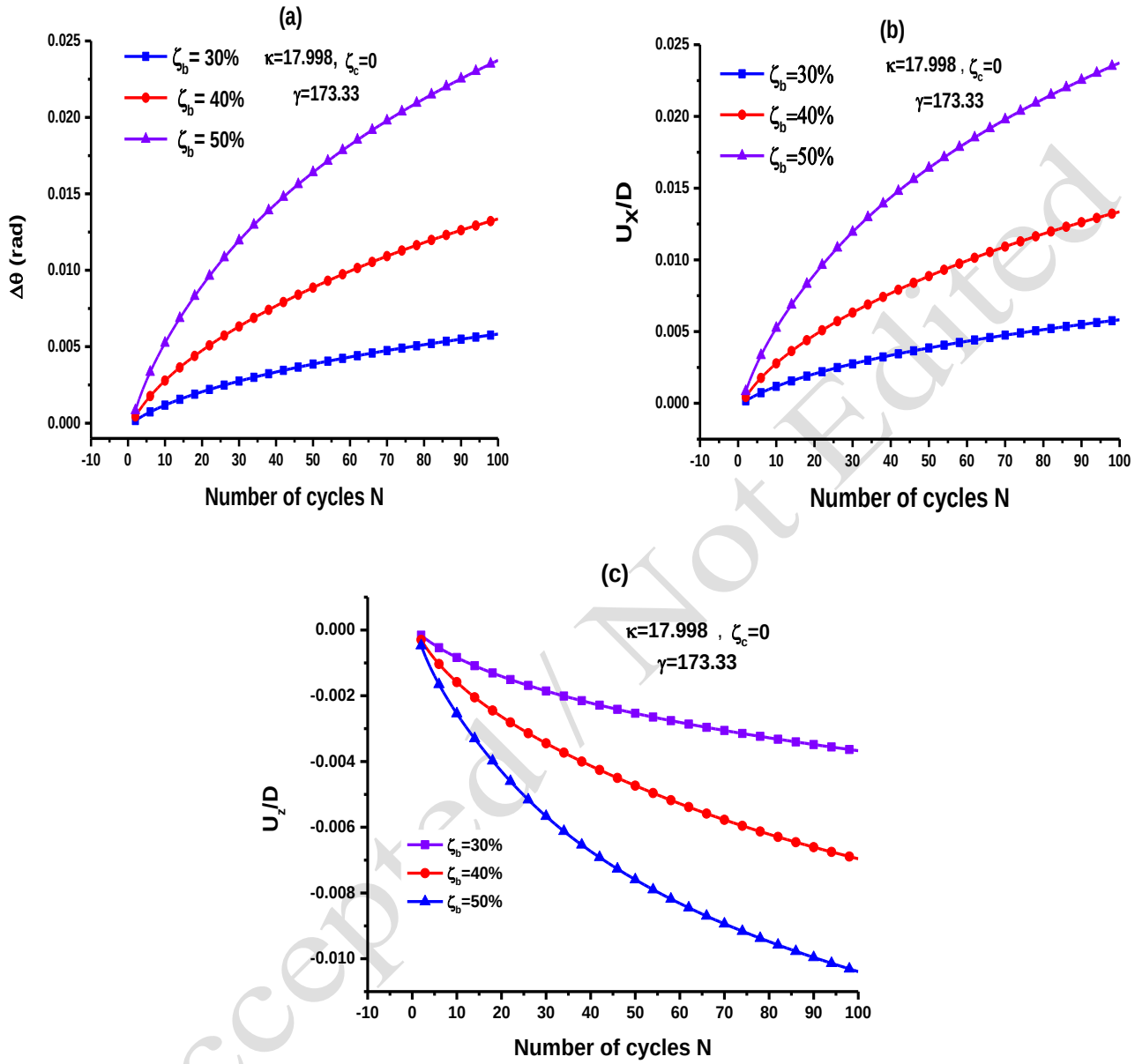

Fig. 13. Effect of cyclic load amplitude ζ_b on cumulative rotations for κ=17.988.

6.3 Effect of cyclic load ratio ζ_c

The variations in cumulative rotations of the bucket foundation subjected to one-way cyclic loading are depicted in Figure 14 (a-d), considering various cyclic load ratio values ζ_c and a range of values of strength non-homogeneity degree κ =10,15,20, and 25, for loading amplitude of 50% from ultimate lateral capacity. The cumulative rotations again exhibited attenuation behavior, characterized by a nonlinear increase with cycling. The amplitude of cumulative rotation was inversely proportional to the cyclic load ratio ζ_c, with maximum cumulative rotations occurring at ζ_c = 0. Additionally, increasing the cyclic load ratio ζ_c from 0 to 0.75 reduces cumulative rotations by approximately 84.86%,89.52%,91.41% and 91.53% for strength non-homogeneity degree κ of 10, 15, 20, and 25, respectively.

Thus, the effect of a higher cyclic load ratio becomes slightly more pronounced as the degree of non-homogeneity rises.

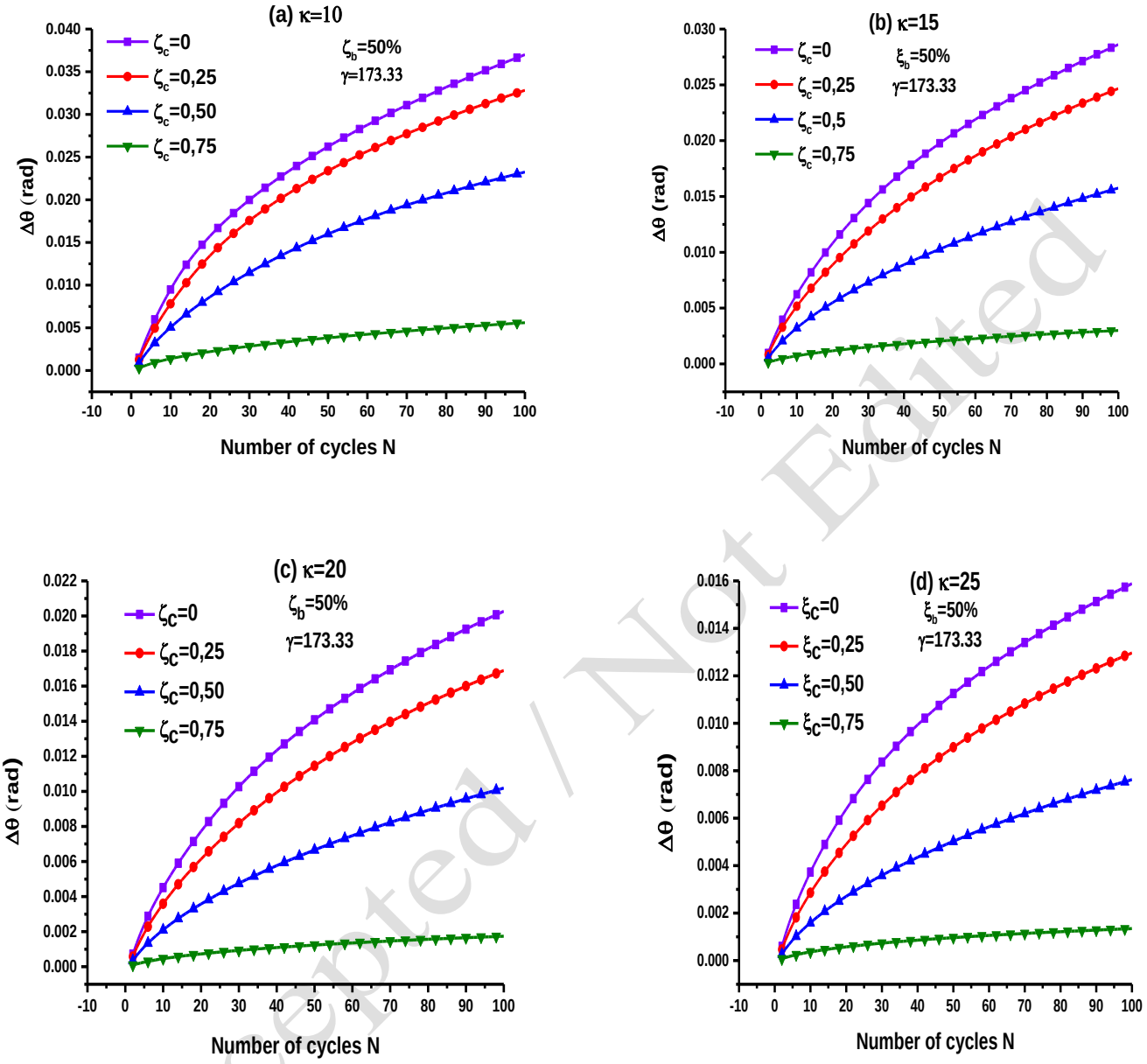

Fig. 14. Effect of cyclic load ratio on cumulative rotation for different values of degree of strength non-homogeneity.

6.4 Effect of the kinematic hardening degradation parameter γ

Figure 15 (a-c) shows the effect of γ, the parameter governing the decay rate of kinematic hardening as plastic deformation accumulates, on the response of the bucket foundation, considering a range of $\gamma = 300$, 500 and 700, with a degree of strength non-homogeneity κ=17.988, loading amplitude ζ_b=50% from ultimate lateral capacity, and a ratio $\frac{\sigma_0}{\sigma_{max}} = 0.1$.

The cumulative rotations and displacements showed a nonlinear increase with cycling, marked by declining slopes that indicated attenuation behavior; this attenuating trend became more pronounced for higher values of the kinematic hardening degradation parameter γ. Quantitatively, the cumulative rotations and displacements were inversely

related to γ. After 100 cycles, the foundation with the lowest γ (γ=300) exhibited the largest rotation of 0.0146 radians. This rotation decreased to 0.0094 and 0.0079 radians for γ=500 and γ=700, respectively.

This trend is a direct consequence of the constitutive role of γ. A higher γ value signifies a more rapid decay of the kinematic hardening modulus. This means the soil's capacity to harden in response to plastic strain diminishes more quickly. Consequently, the soil transitions faster from an initial state of high plastic hardening to a state of saturated hardening, thereby limiting the progressive plastic strain (ratcheting) accumulated per cycle. This results in a stiffer effective cyclic response and, thus, the observed reduction in cumulative displacements.

By increasing the kinematic hardening degradation parameter γ from 300 to 700, the cumulative rotations and both lateral and vertical displacements decrease by about 46.12%, 45.78%, and 50.73 %, respectively. Therefore, an increase in the kinematic hardening degradation parameter γ from 300 to 700 reduces cumulative deformations by approximately 46 to 51%.

Table 5. The lateral capacity for various values of the γ parameter.

γ	Ultimate capacity (kN)
300	8840
500	9000
700	9200

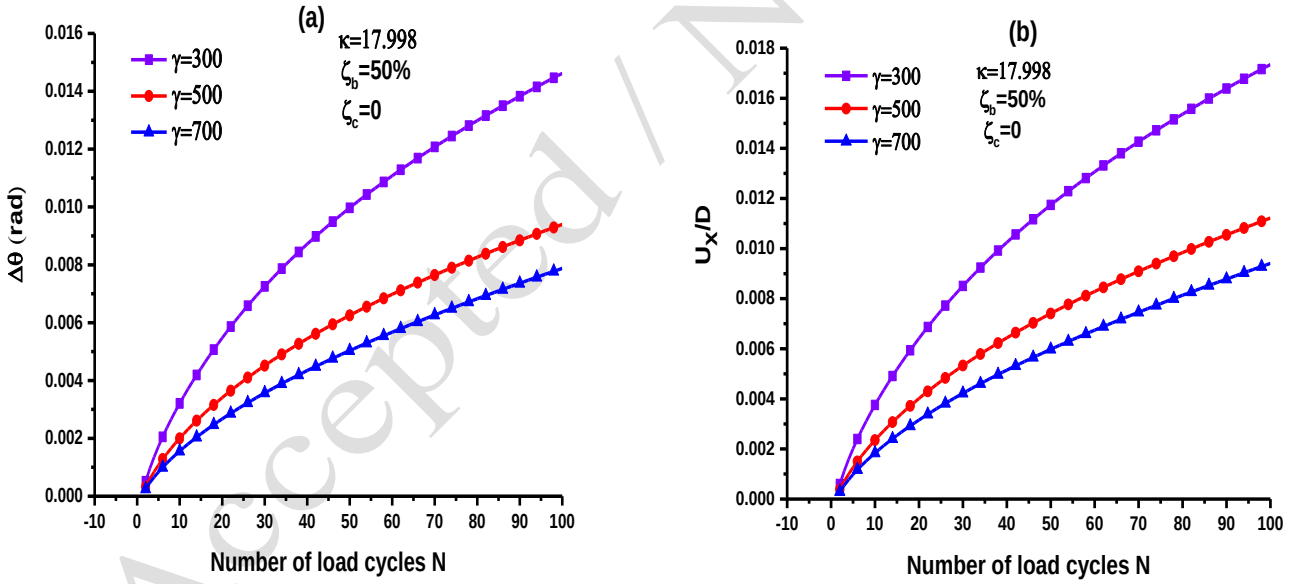

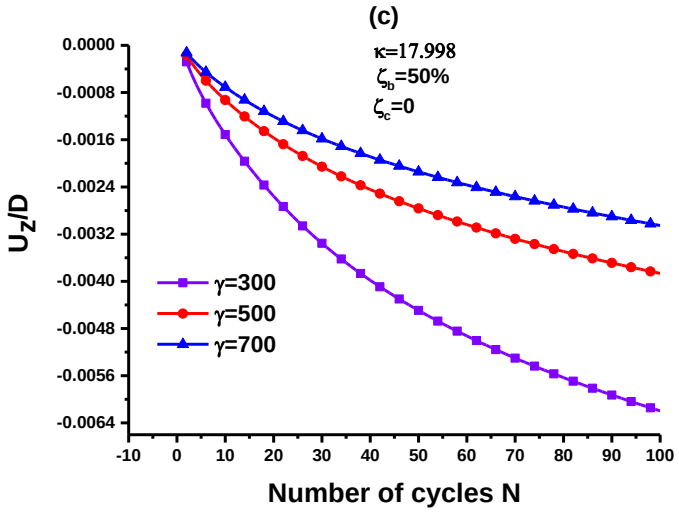

Fig. 15. (a-c) Effect of the kinematic hardening degradation parameter γ on the bucket response.

6.5 Effect of aspect ratio

Figures 16 (a-c) illustrate the influence of the bucket's aspect ratio $\frac{L}{D}$ on the cumulative rotational response for a cyclic load amplitude of ζ_b = 50%. Three aspect ratios were investigated: $\frac{L}{D}$ = 0.5, 0.75, and 1.0.

For a given aspect ratio, cumulative rotations increase nonlinearly with a decaying rate, a clear indication of attenuation behavior. The magnitude of this accumulation is strongly governed by the geometry. For instance, with a strength non-homogeneity of κ = 10, the largest aspect ratio $\frac{L}{D}$ = 1.0 produces the greatest cumulative rotation of 0.0397 rad. This results from a combination of its longer lever arm, which increases the overturning moment, and the higher applied cyclic load, since the load is defined as a fixed percentage ζ_b = 50% of the foundation's larger ultimate capacity. Conversely, a shallower foundation with $\frac{L}{D}$ = 0.5 exhibits a stiffer cyclic response and a significantly lower accumulated rotation of 0.0277 rad.

This trend is consistent across varying soil non-homogeneity, for any fixed aspect ratio, cumulative rotations decrease as the strength non-homogeneity degree κ rises. The analysis confirms that while the fundamental ratcheting and attenuation mechanisms are persistent, the quantitative response is strongly dependent on both geometric $\frac{L}{D}$ and strength non-homogeneity degree κ.

Table 6. The ultimate lateral capacity for different values of aspect ratio $\frac{L}{D}$.

L/D	κ	Ultimate capacity (kN)
0.5	10	3320
	15	4100
	20	4800
	25	5220
0.75	10	5760
	15	7760
	20	9000
	25	10100
1	10	9360
	15	12320
	20	14000
	25	16000

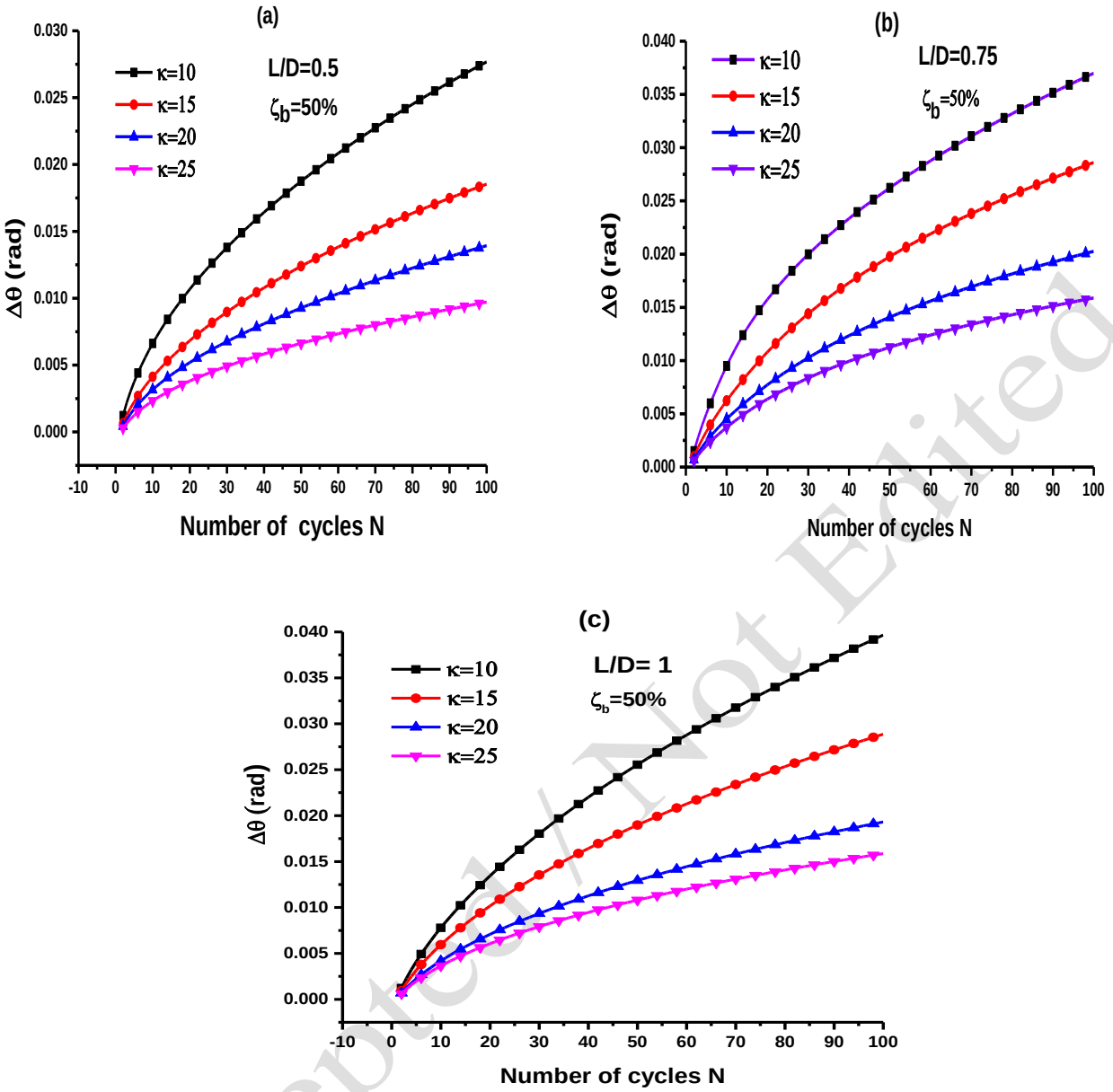

Fig. 16. (a-c) Effect of aspect ratio on the cumulative rotations of the bucket foundation.

7. FEM Implications and Limitations

This study does not account for consolidation, as it models short-term cyclic events under undrained conditions. This undrained assumption is justified because the characteristic time for pore-pressure dissipation in the low-permeability soils considered is orders of magnitude longer than the duration of the applied cyclic loading. Consequently, the modeled soil response is dominated by undrained mechanisms, representing the most conservative case with no dissipation.

For long-duration cyclic loading in the field, partial drainage would likely occur, reducing excess pore pressures and potentially leading to lower cumulative deformations than those predicted in this study.

In reality, under undrained cyclic loading of fine-grained soils, excess pore pressures build up, which tend to diminish the effective stress, soil softening, and potentially cyclic degradation or liquefaction in extreme cases.

For the clayey soil modeled here, the neglect of pore-pressure buildup likely means our results underpredict the gradual accumulation of permanent rotations and displacements of the foundation over 100 cycles.

The use of a symmetry plane, while computationally efficient, simplifies the true

three-dimensional stress field. It enforces a symmetric stress redistribution and precludes the development of asymmetric failure mechanisms or circumferentially non-uniform yielding around the bucket. Thus, the model successfully captures fundamental cyclic plasticity but may not replicate the complete three-dimensional stress field of a real foundation.

Furthermore, the symmetric model may not fully capture the contribution of three-dimensional progressive hardening mechanisms. In reality, out-of-plane confinement and the development of circumferential yield zones could provide additional kinematic constraint, potentially leading to a stiffer cyclic response than predicted here.

8. Conclusion

The present paper investigates the cyclic performance of a suction bucket foundation in clay subjected to one-way cyclic loading through finite element modeling. A nonlinear kinematic hardening model is used in the analyses, available in the ABAQUS code, which is capable of modelling plastic deformations and the consequent ratcheting behavior at cyclic stress levels below the limit state. The analyses were conducted under strictly undrained, non-consolidating conditions. While this approach isolates the effects of cyclic plasticity, it inherently neglects the softening effects of pore-pressure accumulation.

A parametric investigation is conducted to explore the influence of the strength non-homogeneity degree, cyclic load amplitude ζ_b, cyclic load ratio ζ_c, and the kinematic hardening degradation parameter γ.

The results found from this parametric study are presented below:

1. Cumulative rotations and displacements rise nonlinearly with the number of cycles. The accumulation rate is most pronounced during the initial cycles ($N \leq 20$) and undergoes progressive diminution thereafter, characterizing a clear attenuation behavior. Furthermore, the magnitude of these cumulative effects is governed by the soil's strength non-homogeneity κ. The most significant deformations occurred at the lowest κ value. As κ increases, a marked reduction in cumulative rotations and displacements is observed, indicating that a more non-homogeneous strength profile inhibits the ratcheting mechanism, resulting in a stiffer cyclic response. A numerical increase in the strength non-homogeneity degree κ from 10 to 25 leads to significant reductions in cumulative response, with reductions of approximately 57.07% for rotations, 55.60% for lateral displacements, and 74.73% for vertical displacements.
2. Cumulative rotations and displacements increase at a declining rate with the number of load cycles, indicating an attenuating response. This attenuation is primarily due to soil particle rearrangement and densification around the foundation. As expected, the greatest cumulative values occurred under the highest cyclic load amplitude.
3. Cumulative rotations were inversely proportional to the cyclic load ratio, ζ_c, reaching a maximum at $\zeta_c = 0$. Over the investigated range ($\zeta_c = 0$ to 0.75), rotations decreased significantly with increasing ζ_c. The results demonstrate that the influence of ζ_c is slightly mitigated by a higher strength non-homogeneity degree.
4. The magnitude of cumulative rotation and displacement demonstrated an inverse correlation with the kinematic hardening degradation parameter γ. Fundamentally, a higher kinematic hardening degradation parameter value causes rapid hardening saturation by decaying the kinematic modulus faster, thereby inhibiting progressive plastic strain (ratcheting) and producing the observed lower-displacement response. The attenuating trend became more pronounced for higher values of γ.
5. At any fixed aspect ratio, cumulative rotations increase nonlinearly with a decaying rate, a clear manifestation of attenuation behavior. Furthermore, cumulative rotations decrease as the strength non-homogeneity degree κ increases. The analysis confirms that the fundamental ratcheting and attenuation mechanisms are consistent, but their magnitude depends on both bucket geometry (aspect ratio $\frac{L}{D}$) and the soil's strength non-

homogeneity κ.

9. Acknowledgement

The authors acknowledge the use of Grammarly, an AI-based writing assistance tool, to improve the language and clarity of this manuscript.

10. References

Al-Janabi, H. A. and Aubeny, C. P. (2022). "Experimental and numerical investigation of the performance of piles and suction caissons subjected to inclined cyclic loading in cohesive soils", *Journal of Geotechnical and Geoenvironmental Engineering*, 148(6), 04022036, https://doi.org/10.1061/(asce)gt.1943-5606.0002789

Al-Ramthan, A. Q. O. and Aubeny, C. P. (2020). "Numerical investigation of the performance of caissons in cohesive soils under cyclic loading", *International Journal of Geomechanics*, 20(5), 04020042, https://doi.org/10.1061/(asce)gm.1943-5622.0001650

Anastasopoulos, I., Gelagoti, F., Kourkoulis, R. and Gazetas, G. (2011). "Simplified constitutive model for simulation of cyclic response of shallow foundations: validation against laboratory tests", *Journal of Geotechnical and Geoenvironmental Engineering*, 137(12), 1154-1168, https://doi.org/10.1061/(asce)gt.1943-5606.0000534

Andersen, K. H. and Lauritzsen, R. (1988). "Bearing capacity for foundations with cyclic loads", *Journal of Geotechnical Engineering*, 114(5), 540-555, https://doi.org/10.1061/(asce)0733-9410(1988)114:5(540)

Armstrong, P. J. and Frederick, C. O. (1966). "*A mathematical representation of the multiaxial Bauschinger effect*",(Vol. 731): Berkeley Nuclear Laboratories Berkeley, CA. Retrieved February 15, 2026, from https://scholar.google.fr/scholar?hl=fr&as_sdt=0%2C5&q=Armstrong%2C+P.+J.+and+Frederick%2C+C.+O.+%281966%29.+%22A+mathematical+representation+of+the+multiaxial+Bauschinger+effect%22%2C%28Vol.+731%29%3A+Berkeley+Nuclear+Laboratories+Berkeley%2C+CA.&btnG=

Bagheri, P. and Kim, J. M. (2019). "Evaluation of cyclic and monotonic loading behavior of bucket foundations used for offshore wind turbines", *Applied Ocean Research*, 91, 101865, https://doi.org/10.1016/j.apor.2019.101865

Barari, A., Glitrup, K., Christiansen, L. R., Ibsen, L. B. and Choo, Y. W. (2021). "Tripod suction caisson foundations for offshore wind energy and their monotonic and cyclic responses in silty sand: Numerical predictions for centrifuge model tests", *Soil Dynamics and Earthquake Engineering*, 149, 106813, https://doi.org/10.1016/j.soildyn.2021.106813

Chaboche, J.-L. (2008). "A review of some plasticity and viscoplasticity constitutive theories", *International Journal of Plasticity*, 24(10), 1642-1693, https://doi.org/10.1016/j.ijplas.2008.03.009

Chen, C.-H. (2013). "Performance of suction caissons with a small aspect ratio", PhD Thesis, The University of Texas at Austin. http://hdl.handle.net/2152/23092

Cheng, X., Lu, J., Zhuang, Q., El Naggar, M. H., Lu, Q. and Tu, W. (2022). "Lateral cyclic behavior of OWT tripod suction bucket foundation in clays", *Ocean Engineering*, 265, 112635, https://doi.org/10.1016/j.oceaneng.2022.112635

Cheng, X., Wang, P., Li, N., Liu, Z. and Zhou, Y. (2020). "Predicting the cyclic behaviour of suction anchors based on a stiffness degradation model for soft clays", *Computers and Geotechnics*, 122, 103552, https://doi.org/10.1016/j.compgeo.2020.103552

Cheng, X., Yang, A. and Li, G. (2018). "Model tests and finite element analysis for the cyclic deformation process of suction anchors in soft clays", *Ocean Engineering*, 151, 329-341, https://doi.org/10.1016/j.oceaneng.2018.01.027

Debnath, A. and Pal, S. K. (2025). "Behavior of sheet pile wall adjacent to a square and circular footing", *Civil Engineering Infrastructures Journal*, 58(1), 183-201, https://doi.org/10.22059/ceij.2024.368614.1987

Fan, Q.-l., Xiao, G.-f. and Chen, X.-d. (2020). "Analysis of Cyclic Response of Bucket Foundations Based on Simplified Kinematic Hardening Model", *Advances in Civil Engineering*, 2020(1), 9324935, https://doi.org/10.1155/2020/9324935

Feng, X. and Gourvenec, S. (2016). "Modelling sliding resistance of tolerably mobile subsea mudmats", *Géotechnique*, 66(6), 490-499, https://doi.org/10.1680/jgeot.15.p.178

Ghandi, E., Mohammadi Rana, N. and Esmaeili Niari, S. (2025). "Parametric Analysis of Axially Loaded Partially Concrete-Filled Cold-Formed Elliptical Columns Subjected to Lateral Impact Load", *Civil Engineering Infrastructures Journal*, 58(1), 49-70, https://doi.org/10.22059/ceij.2024.364758.1955

Goldscheider, M. and Gudehus, G. (1976). "Einige Bodenmechanische Probleme bei Küsten-und Offshore-Bauwerken", *Vorträge der Baugrundtagung; Deutsche Gesellschaft für Erd- und Grundbau*, Nurnberg, Germany, 507-522,

Houlsby, G., Kelly, R., Huxtable, J. and Byrne, B. (2005). "Field trials of suction caissons in clay for offshore wind turbine foundations", *Géotechnique*, 55(4), 287-296, https://doi.org/10.1680/geot.55.4.287.65487

Hung, L. C., Lee, S.-H., Vicent, S. and Kim, S.-R. (2018). "An experimental investigation of the cyclic response of bucket foundations in soft clay under one-way cyclic horizontal loads", *Applied*

Ocean Research, 71, 59-68, https://doi.org/10.1016/j.apor.2017.11.010

Hydropower and Water Resources Planning Design General Institute, Ministry of Water Resources of China. (2008). "*Design Regulations on Subgrade and Foundation for Wind Turbine Generator System, FD003-2007*", China Water Power Press, Beijing.

Jeong, Y. H., Ko, K. W., Kim, D. S. and Kim, J. H. (2021). "Studies on cyclic behavior of tripod suction bucket foundation system supporting offshore wind turbine using centrifuge model test", *Wind Energy*, 24(5), 515-529, https://doi.org/10.1002/we.2586

Keawsawasvong, S. (2022). "Bearing capacity of conical footings on clays considering combined effects of anisotropy and non-homogeneity", *Ships and Offshore Structures*, 17(10), 2317-2328, https://doi.org/10.1080/17445302.2021.1987110

Kou, H., Fang, W., Zhou, N., Huang, J. and Zhang, X. (2023). "Dynamic response of single-bucket foundation in clay under vertical variable amplitude cyclic loadings", *Ocean Engineering*, 273, 113973, https://doi.org/10.1016/j.oceaneng.2023.113973

Kourkoulis, R., Lekkakis, P., Gelagoti, F. and Kaynia, A. (2014). "Suction caisson foundations for offshore wind turbines subjected to wave and earthquake loading: effect of soil–foundation interface", *Géotechnique*, 64(3), 171-185, https://doi.org/10.1680/geot.12.p.179

LeBlanc, C., Houlsby, G. T. and Byrne, B. W. (2010). "Response of stiff piles in sand to long-term cyclic lateral loading", *Géotechnique*, 60(2), 79-90, https://doi.org/10.1680/geot.7.00196

Lemaitre, J. and Chaboche, J. L. (1990). "Mechanics of solid materials", *UK: Cambridge University Press*, https://doi.org/10.1017/cbo9781139167970

Lian, J., Zhao, Y., Dong, X., Lian, C. and Wang, H. (2021). "An experimental investigation on long-term performance of the wide-shallow bucket foundation model for offshore wind turbine in saturated sand", *Ocean Engineering*, 228, 108921, https://doi.org/10.1016/j.oceaneng.2021.108921

Nielsen, S. D., Ibsen, L. B. and Nielsen, B. N. (2017). "Response of cyclic-loaded bucket foundations in saturated dense sand", *Journal of Geotechnical and Geoenvironmental Engineering*, 143(11), 04017086, https://doi.org/10.1061/(asce)gt.1943-5606.0001787

Ouahab, M. Y., Mabrouki, A., Frank, R., Mellas, M. and Benmeddour, D. (2020). "Undrained bearing capacity of strip footings under inclined load on non-homogeneous clay underlain by a rough rigid base", *Geotechnical and Geological Engineering*, 38, 1733-1745, https://doi.org/10.1007/s10706-019-01127-1

Panwar, V. and Dutta, R. K. (2023). "Development of bearing capacity equation for rectangular footing under inclined loading on layered sand", *Civil Engineering Infrastructures Journal*, 56(1), 173-192, https://doi.org/10.5604/01.3001.0015.5064

Peire, K., Nonneman, H. and Bosschem, E. (2009). "Gravity base foundations for the thornton bank offshore wind farm", *Terra et Aqua*, 115(115), 19-29, Retrieved February 15, 2026, from https://www.iadc-dredging.com/wp-content/uploads/2017/02/article-gravity-base-foundations-for-the-thornton-bank-offshore-wind-farm-115-3.pdf

Roy, A., Liu, H., Bienen, B., Chow, S. and Diambra, A. (2024). "Suction bucket performance in sand under vertical cyclic loading: Numerical modelling using SANISAND-MS", *Computers and Geotechnics*, 173, 106497, https://doi.org/10.1016/j.compgeo.2024.106497

Saleh Asheghabadi, M. and Cheng, X. (2020). "Analysis of undrained seismic behavior of shallow tunnels in soft clay using nonlinear kinematic hardening model", *Applied Sciences*, 10(8), 2834, https://doi.org/10.3390/app10082834

Shen, Z., Pan, Q., Chian, S. C., Gourvenec, S. and Tian, Y. (2021). "Probabilistic failure envelopes of strip foundations on soils with non-stationary characteristics of undrained shear strength", *Géotechnique*, 73(8), 716-735, https://doi.org/10.1680/jgeot.21.00169

Shiva Bhushan, J., Narasimha Reddy, G. and Madhav, M. (2021). "Simple method for the estimation of bearing capacity of footings on non-homogeneous ground", *Paper presented at the Indian Young Geotechnical Engineers Conference*. https://doi.org/10.1007/978-981-97-9831-5_1

Shiva Bhushan, J., Narasimha Reddy, G. and Madhav, M. R. (2023). "Effect of Compressibility on Undrained Bearing Capacity of Circular Embedded Footings Resting on Non-homogeneous Ground", *Indian Geotechnical Journal*, 53(5), 1089-1102, https://doi.org/10.1007/s40098-023-00729-0

Song, C., Tang, X., Wang, K. and Li, M. (2025). "Numerical study of cyclic response of suction bucket interfaces using a three-dimensional critical state model", *Ocean Engineering*, 342, 122964, https://doi.org/10.1016/j.oceaneng.2025.122964

Systèmes, D. (2016). "Abaqus Analysis User's Guide Volume IV: Elements", *Dassault Systèmes Simulia Corp.: Providence, RI, USA*. Retrieved February 15, 2026, from https://ceae-server.colorado.edu/v2016/books/usb/default.htm?startat=pt04ch17s02aus100.html.

Wang, T., Yu, S.-w., Liu, W.-l., Bao, X.-x. and Liu, J.-w. (2021). "Cyclic bearing mechanism of suction caissons supporting offshore wind turbines in clay", *China Ocean Engineering*, 35, 135-144, https://doi.org/10.1007/s13344-021-0012-5

Wang, X., Li, D. and Li, J. (2022). "Centrifuge modeling and numerical analysis on lateral performance of mono-bucket foundation for offshore wind turbines", *Ocean Engineering*, 259, 111925, https://doi.org/10.1016/j.oceaneng.2022.111925

Xiao, Z., Wang, Y., Liu, Y., Tian, Y., Wang, R., Tao, R. and Wei, X. (2022). "Formulas for Uniaxial

Capacities of Tetrapod Bucket Foundations Considering Group Effects in Undrained Clay", *Applied Sciences*, 12(11), 5353, https://doi.org/10.3390/app12115353

Yilmaz, S. A. and Tasan, H. E. (2022). "A study on the behaviour of offshore suction bucket foundations under cyclic axial compressive loading", *International Journal of Geotechnical Engineering*, 16(8), 934-950, https://doi.org/10.1080/19386362.2021.1995139

Zayed, M., Kim, K., Prabhakaran, A. and Elgamal, A. (2023). "Shake table testing and computational framework for seismic response of utility-scale bucket foundation offshore wind turbines", *Soil Dynamics and Earthquake Engineering*, 171, 107939, https://doi.org/10.1016/j.soildyn.2023.107939

Zhang, B., Kang, H.-l., Zhang, X.-h., Lu, X.-b. and Li, Y.-t. (2020). "On the responses of soil layers surrounding a suction bucket under cyclic loads", *Marine Georesources & Geotechnology*, 38(10), 1141-1150, https://doi.org/10.1080/1064119x.2019.1655818

Zhang, J., Cheng, W., Cheng, X., Wang, P. and Wang, T. (2021). "Seismic responses analysis of suction bucket foundation for offshore wind turbine in clays", *Ocean Engineering*, 232, 109159, https://doi.org/10.1016/j.oceaneng.2021.109159

Zhou, N., Kou, H.-l. and Chen, Q. (2022). "Horizontal cyclic response of bucket caisson for offshore wind turbines in over-consolidated clay", *Applied Ocean Research*, 118, 102973, https://doi.org/10.1016/j.apor.2021.102973

Zhou, W., Guo, Z., Wang, L., Zhang, Y. and Rui, S. (2021). "Numerical model for suction caisson under axial cyclic loadings", *Ocean Engineering*, 240, 109956, https://doi.org/10.1016/j.oceaneng.2021.109956

Zhu, B., Byrne, B. and Houlsby, G. (2013). "Long-term lateral cyclic response of suction caisson foundations in sand", *Journal of Geotechnical and Geoenvironmental Engineering*, 139(1), 73-83, https://doi.org/10.1061/(asce)gt.1943-5606.0000738

Zhu, X., Chen, Z., Guan, Y.-F., Ni, P., Fan, K.-F., Jing, Y.-X. and Yang, C.-J. (2023). "Field test on the mechanism of composite bucket foundation penetrating sandy silt overlying clay", *Ocean Engineering*, 288, 116102, https://doi.org/10.1016/j.oceaneng.2023.116102

Ziegler, H. (1959). "A modification of Prager's hardening rule", *Quarterly of Applied Mathematics*, 17(1), 55-65, https://doi.org/10.1090/qam/104405